Pergamon

Bioorganic & Medicinal Chemistry 7 (1999) 2073–2081

BIOORGANIC & MEDICINAL CHEMISTRY

Mechanism of Hemolysis and Erythrocyte Transformation Caused by Lipogrammistin-A, a Lipophilic and Acylated Cyclic Polyamine from the Skin Secretion of Soapfishes (Grammistidae)

Yoshimasa Kobayashi, Hiroyuki Onuki† and Kazuo Tachibana*

Department of Chemistry, School of Science, The University of Tokyo, Hongo, Bunkyo-ku, Tokyo, 113-0033, Japan

Received 10 March 1999; accepted 7 May 1999

Abstract—The mechanism of hemolysis and erythrocyte transformation caused by lipogrammistin-A (LGA), a lipophilic and acylated cyclic polyamine from the skin secretion of soapfishes (Grammistidae), was investigated. The dependency of hemolysis on the erythrocyte concentration indicated that the amount of membrane-bound LGA required for 50% hemolysis is about 13% of the total phospholipids in erythrocytes on a molar basis. A synthetic analogue which lacked a long alkyl chain exhibited much less activity, suggesting that the alkyl chain is important for membrane-binding. In addition, microscopic observations showed that LGA elicited the invagination of erythrocytes at sublytic concentrations, which makes LGA one of the most potent agents with this transforming activity known to date. Its protonated secondary amino group is responsible for the unequal distribution of LGA in the inner leaflet of the lipid bilayer, which leads to invagination, since acetylation at the amino group markedly reduced the invagination activity. Furthermore, the size of LGA-induced lesions on erythrocyte membrane was estimated to be 7–29 Å based on osmotic protection experiments, where the external addition of isotonic molecules in this size range gradually increased the effective dose of LGA. Based on these lines of evidence, the mode of LGA action on erythrocytes is deduced to be as follows. First, LGA molecules bind to erythrocyte membrane by lipophilicity. Second, the molecules accumulate in the inner leaflet of the lipid bilayer by interaction of their cationic ammonium groups with acidic residues of membrane lipid in the inner surface. This uneven distribution of LGA distorts the bilayer structure, and results in a change in cell shape and consequent small lesions. Third, small solutes permeate through the lesions, which induces an osmotic change across the membrane, which leads to colloid-osmotic rupture. This mode of action of LGA on erythrocytes accompanied by cell invagination is the first reported example for natural defense substances.

Introduction

Certain species of fish (ichthyocrinotoxic species) are known to produce ichthyotoxins for defense against predation.[1–3] Although several species have been reported to secrete toxic mucus from their skin, there have been very few studies of their detailed chemical structures and mechanisms of action. The first of these to be chemically investigated was the cationic surfactant pahutoxin from the boxfish, *Ostracicon lentiginosus*, which is a choline ester of fatty acid.[4,5] A series of its analogues were subsequently reported in the secretions from boxfish and trunkfish. Polypeptide surfactants are the largest group of ichthyocrinotoxins and are the best studied. These include pardaxins from the Moses sole (*Pardachirus pavoninus* and *P. marmoratus*).[6–8] The third largest group is steroid glycosides, including pavoninins and mosesins from the Moses sole (*Pardachirus pavoninus* and *P. marmoratus*).[9–12] All of these toxins have amphiphilic structures, and show characteristics common to detergents.[13]

Soapfishes (Grammistidae) are another well-known ichthyocrinotoxic family. The peptidic ichthyotoxins called grammistins have been reported in four typical Grammistid fishes: *Pogonoperca punctata*, *Grammistes sexlineatus*, *Diploprion bifasciatum*, and *Aulacocephalus temmincki*.[14–16] Recently, several grammistins from *G. sexlineatus* and *P. punctata* have been clarified to be polypeptides, which respectively contain 13–25 amino acid residues.[17,18] They are reported to form amphiphilic α-helices[19] and disrupt the cell membrane.[20]

Key words: Lipogrammistin-A; erythrocyte; shape transformation; colloid-osmotic hemolysis.

* Corresponding author. Tel.: +81-3-5841-4366; fax: +81-3-5841-8380; e-mail: ktachi@chem.s.u-tokyo.ac.jp

† Present address: Marine Biotechnology Institute, Sodeshi, Shimizu, Shizuoka, 424-0037, Japan.

0968-0896/99/$ - see front matter
PII: S0968-0896(99)00128-5

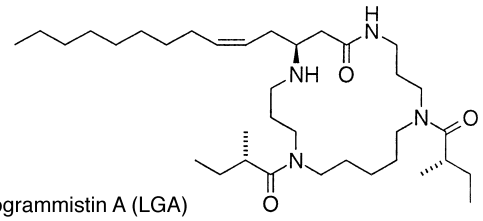

1: Lipogrammistin A (LGA)

In addition to grammistins, the secretions from *D. bifasciatum* and *A. temmincki* have been shown to contain a large amount of lipophilic hemolysin.[16] We recently succeeded in determining the chemical structure of the lipophilic hemolysin, named lipogrammistin-A (LGA, **1**), by spectroscopic methods and total synthesis.[21,22] LGA does not belong to any of the classes of ichthyocrinotoxins described above, and is the first polyamine lactam, as an acylated form, to be isolated from animal sources. Interestingly, LGA was more hydrophobic than other amphiphilic ichthyotoxins, which implies that its mechanism for cytolysis is different than those of detergents.

In this paper, we first report the potent erythrocyte-transformation activity of LGA, and then describe the respective functions of structural components of LGA in its hemolytic and erythrocyte-transformation activities.

Results

Preparation of LGA analogues

An analogue bearing all of the functional groups of LGA except for a long alkyl chain (**2**; Scheme 1) was synthesized by the condensation of *N*-protected β-alanine (**6**) and the acylated polyamine unit of LGA (**5**), synthesis of which has been previously reported.[22] The resulting amide **7** was converted to aldehyde **8** by reduction with $LiBH_4$ and then SO_3-pyridine oxidation. After deprotection, reductive cyclization was carried out via a Schiff base to furnish **2** in modest yield. An *N*-acetyl analogue (**3**; Scheme 2) was prepared from LGA by acetylation with Ac_2O. The structures of analogues **2** and **3** were confirmed by MS and ^1H NMR. An acyclic analogue (**4**; Scheme 2) was derived from LGA by Hofmann degradation,[23] which was carried out by quaternization of its secondary amine with CH_3I. The structure was characterized by MS and by its UV spectrum, which showed the presence of an α,β-unsaturated amide. Its trimethylammonium group was confirmed by ^{13}C NMR of a ^{13}C-labeled derivative of LGA prepared by the same procedure as for analogue **4**, except for using $^{13}CH_3I$.

Membrane affinity and intrinsic hemolytic activity of LGA

Figure 1 shows the dose-dependency of LGA-induced hemolysis for three different densities of erythrocytes. Based on the shift of these curves along the increased density of erythrocytes, the relationship between the bound LGA per cell and percent hemolysis was obtained as shown in Figure 2. The binding isotherm of LGA was also obtained as shown in Figure 3.

Figure 2 shows the intrinsic hemolytic activity of LGA after binding to erythrocytes. Here, the concentration of LGA in erythrocytes required for 50% hemolysis is 5×10^7 molecules/cell, which is estimated to be about 13% of the lipid molecules comprising the membrane of a single cell.[24]

Linearity of the binding isotherm (Fig. 3) implies that LGA is bound as a monomer in the membrane,[25] where

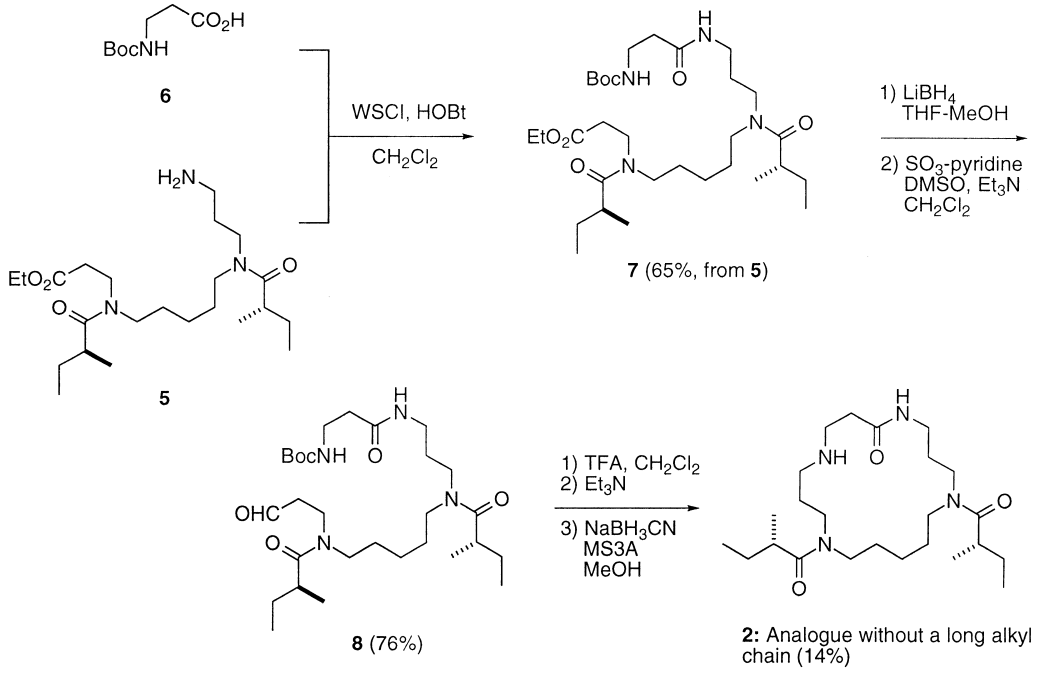

Scheme 1.

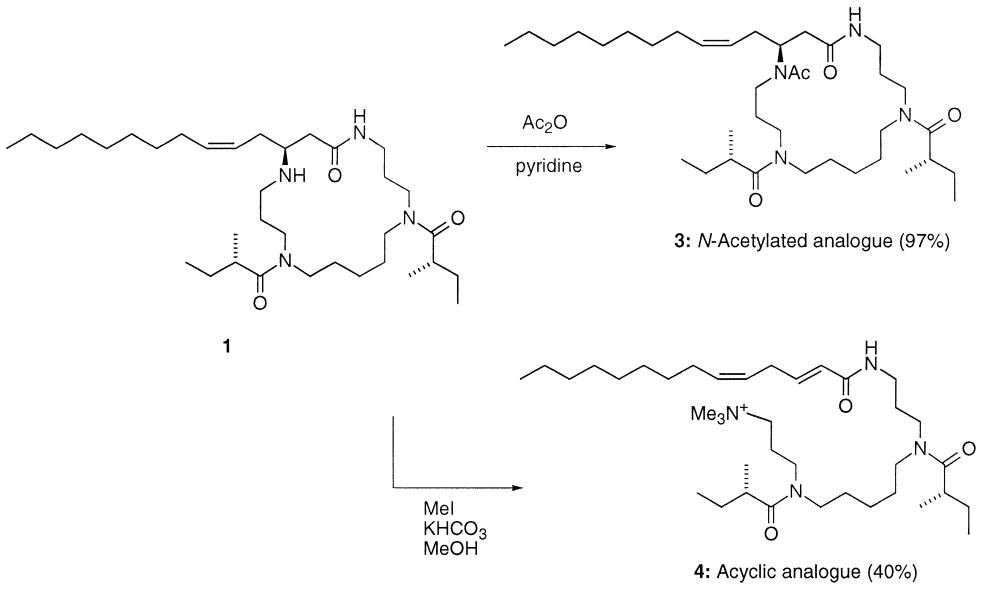

Scheme 2.

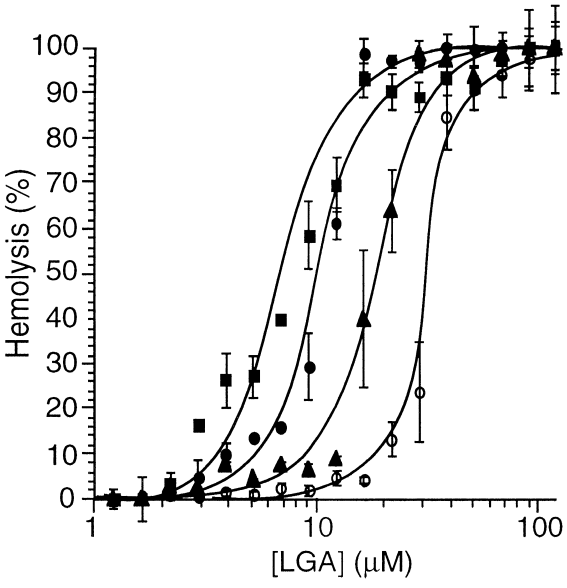

Figure 1. Dose–response curves for LGA-induced hemolysis at an erythrocyte density of 1×10^7 cells/mL (squares), 2×10^7 cells/mL (closed circles), 4×10^7 cells/mL (triangles), and 8×10^7 cells/mL (open circles), mean ± SD, $n=4$. Cells were incubated with LGA at 37°C for 12 h. Other conditions were as in Experimental.

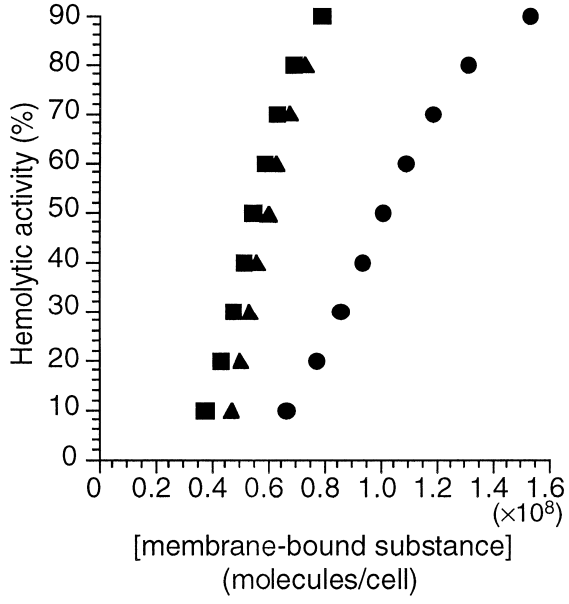

Figure 2. Relationships between the percentage of hemolysis and the amount of membrane-bound substances; LGA (**1**; squares), *N*-acetylated analogue (**3**; circles), and ring-cleaved analogue (**4**; triangles).

most of the molecules incorporated in erythrocytes are presumed to be partitioned. If LGA formed aggregates in the membrane, the binding isotherm would follow an exponential function, considering that LGA should be monomeric in the outer medium at this concentration range. The partition coefficient of LGA from the aqueous medium to cell membrane of erythrocytes is estimated from Figure 3 as 7×10^4 when the avarage volume of the lipid bilayer in an erythrocyte cell is assumed to be 5×10^{-16} L. This can be converted to the association constant (K_a) between LGA and lipid molecule (4×10^8 molecules/cell) as 5×10^4 M^{-1}.

Membrane-perturbing activity of LGA in erythrocytes and SUVs

To estimate the contribution of the membrane-perturbing activity of LGA to hemolysis, LGA-induced fluorescence leakage from calcein-encapsulating SUVs (small unilamellar vesicles) consisting of eggPC (egg-yolk phosphatidylcholine) was evaluated and compared with LGA-induced hemolysis. The dependence of fluorescence leakage on the concentration of LGA is shown in Figure 4 together with hemolysis at the same lipid density for comparison. As shown, these two dose–response curves are very close. As with hemolytic activity,

thermodynamic analysis revealed that two factors, i.e. intrinsic membrane-disrupting activity and membrane-binding affinity, made independent contributions (data not shown). In the case of eggPC-SUV, the association constant K_a was shown to be 1.5×10^5 M^{-1}, which is somewhat higher but at the same magnitude as that obtained for hemolysis. In addition, the concentration of LGA molecules in membrane required for the 50% leakage of calcein was about 20% of the lipid molecules. This value is also close to that obtained for hemolysis. These results indicate that LGA-induced hemolysis is caused not by interaction with membrane-bound proteins, but essentially by membrane disruption.

Transformation of the shape of erythrocytes by LGA

To investigate the mode of action of LGA on erythrocyte membranes in further detail, we examined the shape-transforming activity of LGA on erythrocytes at sublytic doses. Microscopic observation of LGA-treated cells showed that LGA changed the shapes of erythrocytes from normal discoid to an invaginated form (stomatocytes) at 2–3 μM (Fig. 5). At higher doses of LGA, swollen spherical cells (spherocytes) and lysed erythrocytes (i.e. ghosts) were observed. Figure 6 shows the dose-dependency of the LGA-induced shape change. This activity of LGA was compared with that of chlorpromazine, which was previously reported to be a potent erythrocyte-invagination inducer.[26] LGA was one order of magnitude more potent than chlorpromazine on a molar basis.

Size of LGA-induced lesions on erythrocyte membrane

To evaluate the size of the lesions induced by LGA on erythrocyte membrane, osmotic protection experiments were performed. When the lesions are smaller than hemoglobin, a colloid-osmotic process is involved in hemolysis, which can be prevented by adding solutes larger than the lesions to the medium.[27]

Figure 7 shows LGA-induced hemolysis in the presence of osmotic protectants of various sizes. Hemolysis was not prevented by mannitol, but was prevented by substances larger in diameter than PEG 400 (polyethylene glycol 400); PEG 2000 (polyethylene glycol 2000) almost completely prevented lysis at the dose for 100% hemolysis

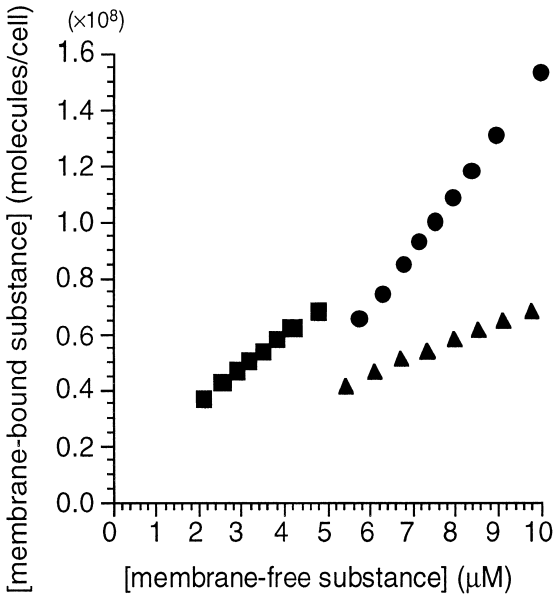

Figure 3. Binding isotherms of LGA (squares), *N*-acetylated analogue (**3**) (circles), and ring-cleaved analogue (**4**) (triangles), where partitions between membrane-bound substances and free substances are shown at different percentages of hemolysis.

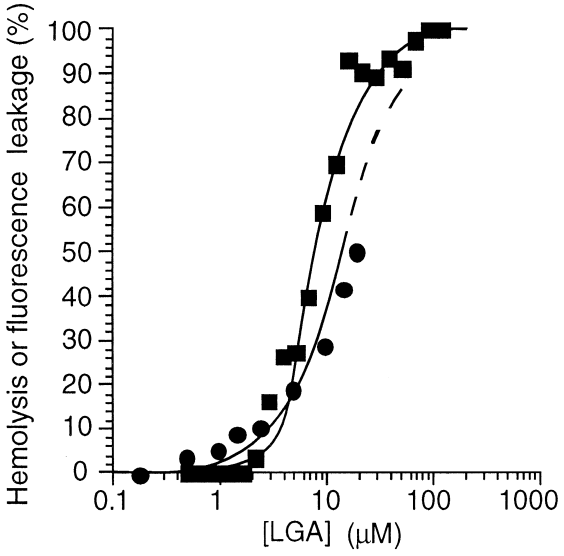

Figure 4. Comparison of the dose–response curve for calcein leakage from liposomes and that for hemolysis; hemolysis induced by LGA (squares), $n=4$, and calcein leakage induced by LGA (circles), $n=2$. Erythrocytes were suspended in buffer at a density of 12 μM EggPC equivalent. Liposomes were diluted to a concentration of 12 μM EggPC equivalent. Other conditions were as in Experimental. Leakage was measured 2 min after a sample was added.

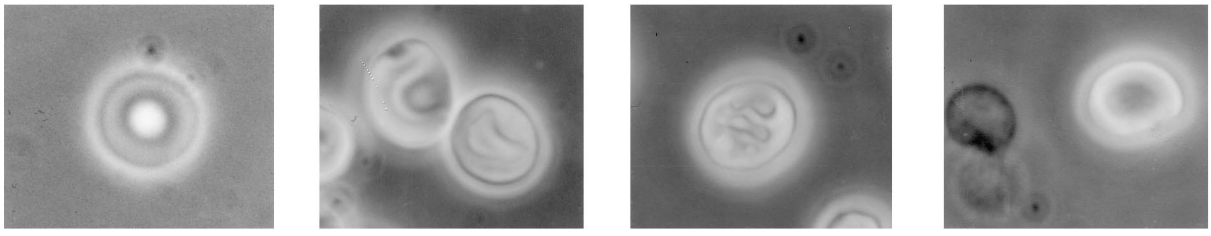

Figure 5. LGA-induced shape changes in erythrocytes. Erythrocytes were incubated for 1 h without (a) and with (b) 3.1 μM. (c) 5.5 μM. (d) 13.1 μM of LGA. Pictures were photographed under a phase-contrast microscope after being fixed with glutaraldehyde.

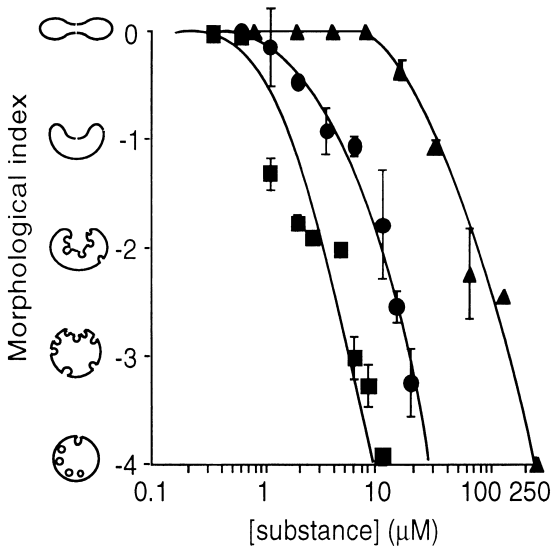

Figure 6. Dose-dependency of changes in erythrocyte shape induced by LGA (squares), *N*-acetylated analogue **3** (circles), and chlorpromazine (triangles). Erythrocytes were suspended in Tris–HCl buffer at a density of 1×10^7 cells/mL. After incubation for 1 h, cells were observed as in Experimental. The extent of transformation was quantified using the morphological index defined by Fujii and co-workers: $\sum$ (negative morphological score) × (number of transformed cells)/(total cell number).[26] Morphological scores of −1 to −4 were assigned to the shapes shown along the vertical axis (mean ± SD, $n=3$).

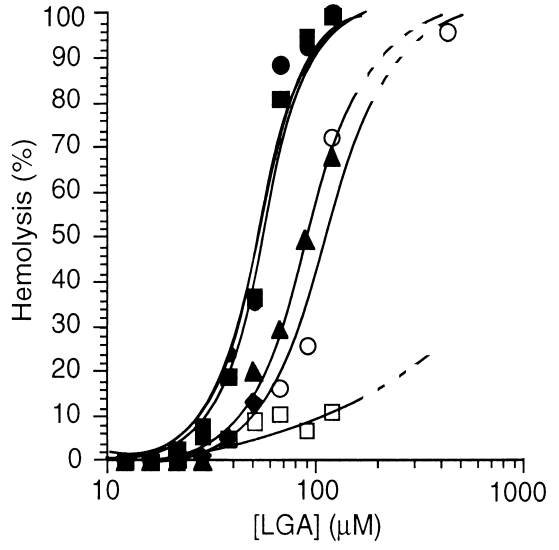

Figure 7. Prevention of hemolysis induced by LGA in the presence of 30 mM various colloid-osmotic protectants; none (closed squares), mannitol (7 Å in diameter,[27] closed circles), raffinose (11 Å, triangles), PEG 400 (12 Å, open circles), and PEG 2000 (29 Å, open squares), $n=4$. Erythrocytes were suspended in Tris–HCl buffer at a density of 2×10^7 cells/mL. Total osmotic pressure was adjusted by reduction of NaCl. Hemolysis was determined after incubation with LGA at 37°C for 30 min. Other conditions were as in Experimental.

(Fig. 7). These results indicate that the membrane lesion formed by LGA is larger than 7 Å (the diameter of mannitol) and smaller than 29 Å (the diameter of PEG 2000).[27] In addition, the required diameter of the protectant increased with the dose of LGA. This indicates that the size of the lesion increases as the dose of LGA increases.

Structural effects on hemolytic and shape-transforming activity

I: Long alkyl chain of LGA. The chemical structure of LGA is characterized by its (i) long alkyl chain, (ii) secondary amine, and (iii) *N*-acyl cyclic polyamine structure. The contribution of each of these structural features to the hemolytic activity and erythrocyte-transforming activity of LGA was then investigated. The synthetic analogue **2**, which has all of the functional groups of LGA except for its long alkyl chain, and is thus less lipophilic, was subjected to hemolysis and liposome assays. These revealed that **2** is devoid of hemolytic activity, and produced much less dye leakage than LGA (7% leakage at 1 mM of **2**, data not shown).

II: Secondary amine. To examine the effect of the basic secondary amino group of LGA on the above biological activities, *N*-acetyl LGA (**3**), a neutral analogue under physiological conditions, was tested in the same manner as LGA. This non-cationic analogue showed less erythrocyte-transforming activity, as shown in Figure 6. It also showed somewhat less hemolytic activity. The thermodynamic data in Figures 2 and 3 revealed that the membrane affinity of **3** is comparable to that of LGA. Therefore, the reduction in both of the activities is believed to be due to the intrinsic potency of **3** in the membrane. The concentration of **3** in the membrane required for 50% hemolysis is 1×10^8 molecules/cell, which is nearly double that of LGA (Fig. 2)

III: Ring structure. To evaluate the contribution of the cyclic structure of LGA to its activities, an acyclic analogue (**4**) was prepared from LGA by quaternization and consequent Hofmann degradation.[23] The analogue **4** showed lower hemolytic and transformation-inducing activities (data not shown). However, a thermodynamic analysis revealed that this reduction in the activities was not due to intrinsic activities, but to a decrease in membrane-binding affinity (Figs 2 and 3).

Discussion

The present experimental results enable us to deduce how LGA induces hemolysis. The mechanism can be divided into three steps; (i) LGA binds to erythrocyte membrane, where (ii) it induces membrane-distortion and erythrocyte-transformation, which (iii) leads to colloid-osmotic hemolysis. Each step is discussed below.

According to our thermodynamic investigations, common events are involved in hemolysis and fluorescence leakage from liposomes consisting of only phosphatidylcholine. This indicates that hemolysis does not involve specific receptors of LGA or other membrane proteins, but rather nonspecific membrane-permeabilization. The potent activity of LGA also involves its high membrane affinity due to its hydrophobicity. Based on the experiments using the truncated analogue **2**, it appears that the long alkyl chain of LGA mainly contributes to its high membrane affinity. The cyclic structure also contributes to its membrane affinity in some degree.

The present study demonstrated that LGA induces cell transformation with invagination at sublytic doses (Fig. 6). Erythrocyte transformation induced by drugs has often been explained by the 'bilayer couple hypothesis' proposed by Sheetz and Singer;[28] i.e. such shape changes may be due to asymmetric expansion of the lipid bilayer membrane of erythrocytes caused by the selective accumulation of a drug in one of the two leaflets of the bilayer. Cationic drugs such as chlorpromazine tend to reside in the inner half of the bilayer due to Coulombic interaction with the acidic phospholipids on this side. This causes expansion of the inner half of the bilayer and results in the invagination of erythrocytes. Although some membrane components such as cholesterol play roles in protecting the membrane against disruption, LGA induced hemolysis in nearly the same dose as in liposome experiments (Fig. 4). This might be because the membranes of LGA-treated erythrocytes are highly distorted due to the uneven accumulation of LGA molecules.

Since the non-cationic derivative of LGA (**3**) exhibits weaker transformation activity (Fig. 6), LGA-induced transformation can be partly accounted for by the bilayer couple hypothesis. However, analogue **3** still induced an invaginated transformation despite its neutrality. Factors other than the mere bilayer couple hypothesis are needed to explain these results. Concerning erythrocyte transformation by a neutral drug, the involvement of aminophospholipid translocase has been proposed,[29,30] and this may also be the case with analogue **3**; i.e. perturbation of the lipid bilayer induced by **3** causes a much faster flip-flop of membrane lipids, resulting in the loss of their asymmetric distribution in the bilayer. To restore the original lipid distribution, aminophospholipid translocase draws phosphatidylethanolamine or phosphatidylserine from the outer monolayer into the inner layer. Consequently, it causes expansion of the inner half of the bilayer and invaginates the erythrocyte.

Analogue **3** induced the same extent of hemolysis at twice the dose as LGA. This reduction in hemolytic activity may be due to the difference in intrinsic activities caused by membrane-bound molecules, since the membrane-perturbing activity of bound LGA is twice that of the *N*-acetyl analogue **3**. On the other hand, the cyclic structure of LGA is not essential for hemolytic activity, since the intrinsic activity of the acyclic analogue **4** is nearly the same as that of LGA once it binds to the membrane (Figs 2 and 3).

While this invaginating erythrocyte-transformation activity has been widely found in local anesthetics and tranquilizers, most of these show weaker hemolytic and transformation activities against erythrocytes than LGA. Furthermore, only a few examples from natural sources are known,[26,31] and none of them are known to show as potent an invagination-inducing activity as LGA. This potent transforming activity can be mostly accounted for by its high membrane affinity. The number of LGA molecules required to cause this shape change, which is estimated to be 10^7 molecules/cell, is roughly the same as that of chlorpromazine.[32]

Next, osmotic protection experiments revealed that small solutes pass through LGA-induced lesions on the membranes of distorted erythrocytes without producing hemolysis. According to these experiments, the lesions are estimated to be smaller than 30 Å, which is too small to allow hemoglobin to pass through the membrane. This indicates that 'colloid-osmotic hemolysis' occurs on erythrocytes; i.e. since small solutes enter through the small lesions by chemical potential, the osmotic balance between the inside and outside of the cell is lost due to entrapped hemoglobin, resulting in the permeation of water into the cell and consequent explosion of the cell. The cells just before explosion can be observed under a microscope as swollen spherocytes at higher sublytic doses.

The experiments also showed that the size of the membrane lesions increases as the dose of LGA increases. This excludes the possibility that LGA forms pores of a specific diameter on the lipid bilayer, such as in ion channel models. In addition, other experimental results have indicated that, unlike ionophores, LGA molecules do not chelate any charged solutes of physiological abundance (unpublished results); in ion extraction assays,[33] ionic solutes such as K^+, Na^+, Ca^{2+} or Mg^{2+} were not extracted by LGA from water to the organic layer. In experiments with an electrode[34] loading LGA, no potential response was observed against ions such as Cl^-, various ammonium ions, or the metal ions mentioned above. These results suggest that solutes enter not through channels (or by carriers), but through 'defects' on the membrane, which are due to bilayer perturbation caused by LGA.

Recent investigations[35,36] have shown that surfactants show two types of hemolytic activity; i.e. a 'fast' activity in which surfactant molecules that penetrate into the lipid bilayer uproot membrane components by forming mixed micelles with them, resulting in the leakage of hemoglobins out of erythrocytes, and a 'slow' activity, which refers to colloid-osmotic lysis. The lesions produced by LGA are smaller than 30 Å even at the dose for 100% hemolysis, since PEG 2000 almost completely protected against lysis (Fig. 7), which shows that lysis is mostly due to the latter activity. The fact that the 'fast' activity does not play a role here may be ascribed to the structure of the LGA molecule, which lacks a distinct amphiphilic nature to solubilize membrane components into micelles. In addition, it might also be ascribed to the shape of the LGA molecule, which is not considered to be suitable for micelle packing.

Thus, the mode of action of LGA on erythrocytes can be summarized as follows. First, LGA monomers are efficiently partitioned to the erythrocyte cell membrane due to their hydrophobic structure. Second, LGA molecules accumulate in the inner leaflet of the lipid bilayer due to electrostatic interaction between their protonated amino groups and the anionic polar heads of membrane lipids, and then distort the bilayer structure to transform the cell shape and create small lesions. Third, small solutes enter through these lesions, which leads to an osmotic imbalance across the membrane.

Consequently, the erythrocytes undergo colloid-osmotic lysis. This mode of action of LGA on erythrocytes accompanied by cell invagination is the first reported example for natural defense substances.

Experimental

Chemistry

General methods. $^{13}CH_3I$ was purchased from Shoko Tsusho, Tokyo, Japan. All other chemicals were purchased from Kanto Chemicals, Tokyo, Japan. NMR spectra were recorded on a Bruker AM-500 spectrometer at 500 MHz for ^1H, 125 MHz for ^{13}C with $C\underline{H}Cl_3$ at 7.24 ppm, $C\underline{H}D_2OD$ at 3.30 ppm, $^{13}\underline{C}DCl_3$ at 77.0 ppm, or $^{13}\underline{C}D_3OD$ at 49.0 ppm. NMR data are those of equilibrated mixtures of conformers due to amide/urethane bond rotation. Reactions requiring anhydrous conditions were carried out in dry, freshly distilled solvents under a nitrogen or argon atmosphere.

Isolation and purification of LGA (1). LGA was isolated from the skin mucus of *Aulacocephalus temmincki*, a species of soapfish (Grammistidae), as reported previously.[21] Briefly, the acetone extract of mucus scraped from the fish skin was partitioned between water and ethyl acetate, and the ethyl acetate layer was fractionated through an alumina column (chloroform:methanol, 98:2 to 92:8) followed by repeated reversed-phase HPLC on ODS to yield LGA (0.5% yield based on wet mucus).

***N*-(*tert*-Butoxycarbonyl)-β-alanine (6).** β-Alanine (1.78 g, 20 mmol) was dissolved in dioxane:H_2O (2:1) (60 mL). To this solution were added 1 M aqueous NaOH (20 mL) and Boc_2O (4.7 mL, 20 mmol). The reaction mixture was stirred at room temperature for 30 min. After evaporation of the solvent, the residue was adjusted to pH 3 with 5% aqueous $KHSO_4$, and extracted with EtOAc. Concentration and recrystallization from hexane–EtOAc afforded **6** (3.25 g, 87%) as white needles: ^1H NMR ($CDCl_3$, 500 MHz) δ 11–8.5 (br, 1H), 3.36 (br, 2H), 2.54 (br, 2H), 1.40 (brs, 9H); ^{13}C NMR ($CDCl_3$, 125 MHz) 177.4, 156.0, 79.7, 35.9, 34.4, 28.3.

Ethyl 14-[*N*-(*tert*-butoxycarbonyl)-β-alanyl]-4,10-bis[(2*S*)-2-methylbutyryl]-4,10,14-triazatetradecanoate (7). To a solution of crude **5**·HCl (41.9 mg, 0.090 mmol) in dry CH_2Cl_2 (2 mL) were added Et_3N (15 mL, 0.11 mmol), HOBt (21 mg, 0.14 mmol), WSCI (30 mg, 0.16 mmol), and *N*-Boc-β-alanine (**6**) (23 mg, 0.12 mmol). After stirring at room temperature overnight, the solvent was evaporated. The crude residue was dissolved in EtOAc, and washed successively with 5% aqueous $KHSO_4$, saturated aqueous $NaHCO_3$, and brine. Concentration and column chromatography of the residue on silica gel (2 g, $CHCl_3$:MeOH, 98:2) afforded **7** (35.3 mg, 65%) as a colorless oil: $[\alpha]_D^{27}+15.0°$ (*c* 0.753, $CHCl_3$); IR (film) 3315, 1732, 1713, 1641, 1633 cm^{-1}; ^1H NMR ($CDCl_3$, 270 MHz) δ 7.03 (br, 1H), 4.13 and 4.09 (each q, 2H, $J=7.0$ Hz), 3.57 (m, 2H), 3.42–3.07 (m, 10H), 2.57 and 2.53 (each t, 2H, $J=7$ Hz), 2.60–2.42 (m, 2H), 2.38 (t, 2H, $J=7$ Hz), 1.70–1.50 (m, 8H), 1.39 (s, 9H), 1.25 (m, 2H), 1.25 and 1.21 (each t, 3H, $J=7.0$ Hz), 1.07 (m, 6H), 0.85 (m, 6H).

14-[*N*-(*tert*-Butoxycarbonyl)-β-alanyl]-4,10-bis[(2*S*)-2-methylbutyryl]-4,10,14-triazatetradecanal (8). To a solution of **7** (320 mg, 0.535 mmol) in THF (15 mL) and MeOH (0.1 mL) was added $LiBH_4$ (60 mg, 2.8 mmol). After stirring at room temperature overnight, 1 M aqueous potassium sodium tartrate (30 mL) was added. Extraction with $CHCl_3$ and concentration afforded a crude residue, which was then dissolved in dry CH_2Cl_2 (10 mL) and DMSO (5 mL). To this solution were added Et_3N (0.59 mL, 4.2 mmol) and SO_3-pyridine complex (307 mg, 1.93 mmol) at 0°C. After stirring at 0°C for 2 h and then at room temperature for 1 h, the reaction mixture was diluted with EtOAc (30 mL), and washed successively with H_2O, 5% aqueous $KHSO_4$, saturated aqueous $NaHCO_3$, and brine. Concentration and flash chromatography on silica gel (10 g, $CHCl_3$:MeOH, 95:5) afforded 225.4 mg (76%) of **8** as a colorless oil: $[\alpha]_D^{24}+23.4°$ (*c* 1.39, MeOH); IR (film) 3315, 1710, 1625 cm^{-1}; ^1H NMR ($CDCl_3$, 500 MHz) δ 9.7–9.6 (m, 1H), 7.2–7.0 (br, 1H), 5.4–5.3 (br, 1H), 3.62–3.30 (m, 12H), 2.77–2.60 (m, 2H), 2.55–2.40 (m, 2H), 2.35 (m, 2H), 1.80–1.45 (m, 8H), 1.36 (m, 2H), 1.35 (brs, 9H), 1.02 (m, 6H), 0.80 (m, 6H); ^{13}C NMR ($CDCl_3$, 125 MHz) 200.8, 199.4, 177.6, 176.8, 176.5, 176.5, 171.7, 156.0, 79.0, 48.4, 47.3, 45.5, 43.9, 43.0, 42.4, 40.5, 37.4, 37.3, 37.3, 37.2, 36.8, 36.2, 35.5, 29.6, 29.4, 29.2, 28.4, 27.3, 27.3, 24.1, 18.0, 17.9, 17.8, 17.7, 12.1, 12.1, 12.0.

8,14-Bis[(2*S*)-2-methylbutyryl]-4,8,14-triaza-17-heptadecanolactam (2). A solution of aldehyde **8** (28.9 mg, 0.052 mmol) in dry CH_2Cl_2 (1 mL) and TFA (1 mL) was stirred at room temperature for 20 min. After removal of the solvents, the residue was dissolved in dry MeOH (10 mL). MS3A (1 g) and Et_3N (14 mL) were added to give pH 7. After stirring at room temperature for 45 min, $NaBH_3CN$ (12 mg, 0.19 mmol) was added. The mixture was stirred at room temperature overnight, and filtered through a Celite pad, followed by the addition of saturated aqueous $NaHCO_3$. After insoluble materials were filtered off, the reaction mixture was dried over Na_2SO_4, and the concentrated crude product was chromatographed through an alumina column (neutral, activity II, 10 g, $CHCl_3$:MeOH, 9:1) and further purified by HPLC (SiO_2, YMC A-024, $CHCl_3$:MeOH:*i*-$PrNH_2$, 9:1:0.2) to afford 3.0 mg (14%) of **2** as a colorless oil: ^1H NMR ($CDCl_3$, 500 MHz) δ 4.09 and 3.99 (q each, 2H, $J=7$ Hz), 3.45 (m, 2H), 3.40 (m, 2H), 3.35–3.13 (m, 4H), 2.58 (m, 2H), 2.54–2.36 (m, 2H), 1.63–1.40 (m, 6H), 1.30 (m, 2H), 1.20 (m, 2H), 1.15 and 1.12 (t each, 3H, $J=7$ Hz), 0.97 (m, 6H), 0.74 (m, 6H); MS (EI) *m*/*z* (rel. intensity) 438 (32), 423 (7), 381 (13), 353 (100), 57 (87); HRMS (EI) *m*/*z* calcd for $C_{24}H_{46}N_4O_3$ (M^+) 438.3570, found 438.3610.

Preparation of acetylated analogue (3) from LGA. To a solution of LGA (295 μg, 0.5 μmol) in dry pyridine (250 μL) was added Ac_2O (10 μL, 100 μmol) at 0°C. After stirring at room temperature for 15 h, complete removal of the solvent and flash chromatography on silica gel (100 mg, $CHCl_3$:MeOH, 95:5) afforded 308 μg (97%) of **3** as a yellow oil. HRMS (FAB, 3-nitrobenzylalcohol matrix) *m*/*z* calcd for $C_{37}H_{69}N_4O_4$ ($[M+H]^+$) 633.5319, found 633.5292. Acetyl signals in ^1H NMR of the acetyl

group (CD_3OD, 500 MHz) δ 2.12 (s), 2.15 (s), 2.20 (s), 2.22 (s), 2.48 (s), 2.50 (s), 2.54 (s), 2.55 (s). This signal multiplication is due to restricted rotation around three tertiary amide groups, since mutual saturation transfers were observed among these signals.

Preparation of acyclic analogue (4) from LGA. To a solution of LGA (301 μg, 0.5 μmol) in dry MeOH was added $KHCO_3$ (2 mg, 20 μmol), and then CH_3I (5 μL, 80 μmol) slowly at 0°C. After stirring under darkness at room temperature overnight, the reaction mixture was concentrated, and $CHCl_3$ extract was subjected to flash chromatography on silica gel (100 mg, $CHCl_3$:MeOH: *i*-PrOH, 15:5:1) and further purified by HPLC (ODS, YMC AM-323, CH_3CN:H_2O:TFA, 60:40:0.05) to give 170 μg (40%) of **4** as a TFA salt. HRMS (FAB, 3-nitrobenzylalcohol matrix) *m*/*z* calcd for $C_{38}H_{73}N_4O_3$ (M^+) 633.5683, found 633.5710. UV (MeOH) λ_{max} 208 nm, ($\varepsilon = 9.0\times10^3$), α,β-unsaturated amide. For the analogue obtained using $^{13}CH_3I$, a tri-^{13}C-methyl ammonium group was characterized in the ^{13}C NMR spectrum (CD_3OD, 125 MHz) δ 53.5 (brs).

Biological assay

Materials and instruments. EggPC was purchased from Sigma, MO, USA. Calcein and EDTA were purchased form Dojindo, Kumamoto, Japan. Polyethylene glycol mono-*p*-octaphenyl ether was purchased from Tokyo Chemical Industry, Tokyo, Japan. All other chemicals were purchased from Kanto Chemicals, Tokyo, Japan. Fluorescence was recorded on a Hitachi 650-60 spectrophotometer. Cell morphology was observed under a phase-contrast microscope, OLYMPUS BX-40.

Erythrocytes. Freshly drawn, heparinized human blood was washed three times with Tris–HCl buffer (150 mM NaCl, 10 mM Tris/HCl, 1 mM EDTA, 22 mM glucose, pH 7.4) to remove plasma and buffy coat. In each experiment, the erythrocytes were washed more than two times with the same buffer and resuspended in it. The cell density was determined by visually counting the cells in 0.01 μL of the suspension under a light microscope.

Preparation of liposomes. SUVs were prepared from a lipid film of EggPC that had been thoroughly dried in vacuo and then hydrated with the Tris–HCl buffer containing 60 mM calcein. After vortex mixing and ultrasonication at 0°C under a nitrogen stream for 60 min, the resultant SUVs were separated from untrapped calcein and multilamellar vesicles by gel filtration (Sepharose 4B, 2×40 cm, 10 mM Tris–HCl buffer solution with 150 mM NaCl and 1 mM EDTA as an eluent).

Measurements of fluorescence leakage. An aliquot of the SUV suspension was diluted with 2 mL of the Tris–HCl buffer to a certain lipid concentration in a 3-mL cuvette for fluorescence measurements. After the addition of a sample solution in 10 μL of MeOH, calcein leakage from SUVs was monitored fluorometrically (excitation at 490 nm and emission at 520 nm). The fluorescence increase reached a plateau within 2 min in all cases. The fluorescence intensity obtained by the addition of 20 μL of a solution of 10% (v/v) polyethylene glycol mono-*p*-octaphenyl ether was taken as 100% leakage.

Hemolysis tests. After erythrocytes were diluted with the same buffer as in Erythrocytes to a known concentration, 1.25 μL of a solution of the tested substance in MeOH was added to a 200-μL aliquot of the suspension. Cells were incubated at 37°C and sedimented by centrifugation, and then 100 μL of the supernatant was transferred for measurement of the concentration of hemoglobin at 420 or 540 nm. One hundred percent hemolysis was obtained by incubating the cells with a greater than 20-fold volume of distilled water for the same period. The sediments were subjected to the morphological observations described below.

Thermodynamic analysis of hemolysis. Dose-dependence curves for substance-induced hemolysis of erythrocytes at different cell densities may reflect not only the intrinsic hemolytic activity of the added sample but also the degree of its distribution in the cells. To evaluate the intrinsic hemolytic efficacy of a substance that is assumed to be incorporated equally into cells, the following calculations were applied.[12,25,37] The material balance equation is:

$$[S]_t = [S]_f + [S]_b = [S]_f + r[\text{erythrocyte}]$$

where the total concentration of added substance, $[S]_t$, consists of the fraction in the test media, $[S]_f$, and the cell-bound fraction, $[S]_b$, at the specific erythrocyte density, [erythrocyte]. On the assumption that the percentage of hemolysis is determined solely by the average bound amount of substance molecules per cell, $r = \frac{[S]_b}{[\text{erythrocyte}]}$, linearity between $[S]_t$ and [erythrocyte] is expected at any given percentage of hemolysis. Since $[S]_t$ and [erythrocyte] are measurable, the values *r* and $[S]_f$ can be obtained as the slope and intercept, respectively, by plotting the $[S]_t$ required for each percentage of hemolysis against [erythrocyte]. Thus, the relationship between *r* and the percentage hemolysis can be obtained as the intrinsic hemolytic activity of a substance against [erythrocyte]. The relationship between *r* and $[S]_f$, which is known as the binding isotherm, can be obtained in the same manner. The partition coefficient is obtained from the slope of the binding isotherm ($= \frac{r}{[S]_f}$) by converting the unit of *r* to molarity in erythrocyte membrane.

Morphological observation of erythrocytes undergoing lysis. To a small amount (ca. 5 μL) of the erythrocyte suspension was added 5 μL of 0.9% glutaraldehyde solution in Tris–HCl buffer (150 mM NaCl, 10 mM Tris/HCl, 1 mM EDTA, 22 mM glucose, pH 7.4). The fixed erythrocytes were observed microscopically. The changes in the shapes of erythrocytes were quantified using the morphological index defined by Fujii and coworkers.[26]

Acknowledgements

The authors gratefully acknowledge Professor Y. Umezawa and Dr K. Tohda in their department and Professor M. Sugawara, Nihon University, Tokyo, Japan,

who allowed us to use their equipment and provided helpful suggestions. The authors are also grateful to Professor M. Murata, Osaka University, Osaka, Japan, for his valuable discussion and critical reading of this manuscript.

References

1. Tachibana, K. In *Bioorganic Marine Chemistry*; Scheuer, P. J., Ed.; Springer-Verlag: Berlin, 1988; Vol. 2, pp. 117–138.
2. Nair, M. S. R. In *Handbook of Natural Toxins*; Tu, A. T., Ed.; Marcel Dekker: New York, 1988; Vol. 3, pp. 211–226.
3. Hashimoto, Y. *Marine Toxins and Other Bioactive Marine Metabolites*; Japan Scientific Societies Press: Tokyo, 1979; pp. 312–332.
4. Boylan, D. B.; Scheuer, P. J. *Science* **1967**, *155*, 52–56.
5. Yoshikawa, M.; Sugimura, T.; Tai, A. *Agric. Biol. Chem.* **1989**, *53*, 37–40.
6. Thompson, S. A.; Tachibana, K.; Nakanishi, K.; Kubota, I. *Science* **1986**, *233*, 341–343.
7. Thompson, S. A.; Tachibana, K.; Kubota, I.; Zlotkin, E. In *Peptide Chemisty 1987*; Shiba, T.; Sakakibara, S., Eds.; Protein Research Foundation: Osaka, 1988; pp. 127–132.
8. Shai, Y. *Toxicology* **1994**, *87*, 109–129.
9. Tachibana, K.; Sakaitani, M.; Nakanishi, K. *Science* **1984**, *226*, 703–705.
10. Tachibana, K.; Sakaitani, M.; Nakanishi, K. *Tetrahedron* **1985**, *41*, 1027–1038.
11. Tachibana, K.; Gruber, S. H. *Toxicon* **1988**, *26*, 839–853.
12. Ohnishi, Y.; Tachibana, K. *Bioorg. Med. Chem.* **1997**, *5*, 2251–2265.
13. Abdul-Haqq, A. J.; Shier, W. T. *J. Toxicol., Toxin Rev.* **1991**, *10*, 289–320.
14. Hashimoto, Y.; Kamiya, H. *Toxicon* **1969**, *7*, 65–70.
15. Randall, J. E.; Aida, K.; Hibiya, T.; Mitsuura, N.; Kamiya, H.; Hashimoto, Y. *Publ. Seto Mar. Bio. Lab.* **1971**, *19*, 157–190.
16. Oshima, Y.; Shiomi, K.; Hashimoto, Y. *Bull. Jpn. Soc. Sci. Fish.* **1974**, *40*, 223–230.
17. Shiomi, K.; Igarashi, T.; Shimakura, K.; Nagashima, Y. *Spring meeting of the Japanese Society of Fisheries Science*, Tokyo, 1997, Abstract 1005.
18. Yokota, H.; Shimakura, K.; Nagashima, Y.; Shiomi, K. *Spring meeting of the Japanese Society of Fisheries Science*, Tokyo, 1998, Abstract 1054.
19. Shiomi, K.; Igarashi, T.; Shimakura, K.; Nagashima, Y. *Autumn meeting of the Japanese Society of Fisheries Science*, Hiroshima, 1997, Abstract 832.
20. Yokota, H.; Shimakura, K.; Nagashima, Y.; Shiomi, K. *Autumn meeting of the Japanese Society of Fisheries Science*, Hakodate, 1998, Abstract 823.
21. Onuki, H.; Tachibana, K.; Fusetani, N. *Tetrahedron Lett.* **1993**, *34*, 5609–5612.
22. Onuki, H.; Ito, K.; Kobayashi, Y.; Matsumori, N.; Tachibana, K.; Fusetani, N. *J. Org. Chem.* **1998**, *63*, 3925–3932.
23. Chen, F. C. M.; Benoiton, N. L. *Can. J. Chem.* **1976**, *54*, 3310–3311.
24. Beutler, E. In *Hematology, 4th ed.* Williams, W. J.; Beutler, E.; Erslev, A. J.; Lichtman, M. A., Eds.; McGraw-Hill: New York, 1990; pp. 317–322.
25. Matsuzaki, K.; Nakai, S.; Handa, T.; Takaishi, Y.; Fujita, T.; Miyajima, K. *Biochemistry* **1989**, *28*, 9392–9398.
26. Fujii, T.; Sato, T.; Tamura, A.; Wakatsuki, M.; Kanaho, Y. *Biochem. Pharmacol.* **1979**, *28*, 613–620.
27. Katsu, T.; Ninomiya, C.; Kuroko, M.; Kobayashi, H.; Hirota, T.; Fujita, Y. *Biochim. Biophys. Acta* **1988**, *939*, 57–63.
28. Sheetz, M. P.; Singer, S. J. *Proc. Natl. Acad. Sci. USA* **1974**, *71*, 4457–4461.
29. Schrier, S. L.; Zachowski, A.; Devaux, P. F. *Blood* **1992**, *79*, 782–786.
30. Loh, R. K.; Huestis, W. H. *Biochemistry* **1993**, *32*, 11722–11726.
31. Thimon, L.; Peypoux, F.; Exbrayat, J. M.; Michel, G. *Cytobios* **1994**, *79*, 69–83.
32. Seeman, P. *Pharmacol. Rev.* **1972**, *24*, 583–655.
33. Moore, S. S.; Tarnowski, T. L.; Newcomb, M.; Cram, D. J. *J. Am. Chem. Soc.* **1977**, *99*, 6398–6405.
34. Ito, T.; Radecka, H.; Tohda, K.; Odashima, K.; Umezawa, Y. *J. Am. Chem. Soc.* **1998**, *120*, 3049–3059.
35. Bielawski, J. *Biochim. Biophys. Acta* **1990**, *1035*, 214–217.
36. Chernitsky, E. A.; Senkovich, O. A. *Membr. Cell Biol.* **1997**, *11*, 475–485.
37. Hu, M.; Konoki, K.; Tachibana, K. *Biochim. Biophys. Acta* **1996**, *1299*, 252–258.